

Supplementary Material: Synchrotron Radiation Photoemission Spectroscopy of Oxygen Modified CrCl₃ Surface

S. Kazim^a, D. Mastrippolito^b, P. Moras^c, M. Jugovac^c, T. Klimczuk^d, M. Ali^{b,e}, L. Ottaviano^{b,f}, R. Gunnella^{a,g,h}

^aPhysics Section, School of Science and Technology, University of Camerino, 62032 Camerino (MC), Italy

^bDipartimento di Scienze Fisiche e Chimiche (DSFC), Università degli Studi dell'Aquila

^cIstituto di Struttura della Materia-CNR (ISM-CNR), SS 14, Km 163,5, 34149 Trieste, Italy.

^dFaculty of Applied Physics and Mathematics, and Advanced Materials Centre, Gdansk University of Technology, ul. Narutowicza 11/12, 80-233 Gdansk, Poland

^eDepartment of Physics, Division of Science and Technology, University of Education Lahore, Jauharabad Campus, Pakistan.

^fCNR-SPIN UoS L'Aquila. Via Vetoio 10 67100 L'Aquila, Italy

^gINFN-Sez. Perugia, Via Pascoli Perugia, Italy

^hCorresponding author: Roberto Gunnella, roberto.gunnella@unicam.it

1. Material preparation:

Starting material details are provided in ref.[1]. Anhydrous chromium(III) chloride (Thermo Scientific) with a purity of 99% was used as a starting material. The powder was stored in an Ar-filled glovebox and XRD characterization is presented in ref.[2]. High-quality single crystals were grown by the self-transport technique, using commercial CrCl₃ powder, that was subjected to an oxygen purification process and then enclosed in a 20 cm quartz tube. The tube was placed in a three-zone furnace with a temperature gradient of about 25°C between the hot and cold zones. The hot end of the furnace was heated to 1000°C, held for an hour at a constant temperature, and then gradually cooled to 700°C at a cooling rate of 3°C/hour. Then the quartz tube was kept at 700°C temperature for 7 days. The grown crystals were stored in a glove box filled with argon gas. The samples were eventually cleaved both in vacuum as well as in air for better experimental comparison [3, 4]. Magnetic characterization is provided in ref.[3], Serri et al. demonstrated the larger antiferromagnetic interaction or anisotropy on exfoliated CrCl₃ (≈ 10 nm thick) by X-ray magnetic circular dichroism (XMCD) and Magnetic force microscopy (MFM) than in bulk.

2. Cl 2p core level spectra taken at 300°C :

The Cl 2p spectra at 300°C consist of more components than at 150°C. As we mentioned in the main text, such extra components are related to the increasing number of vacancies per unit surface.

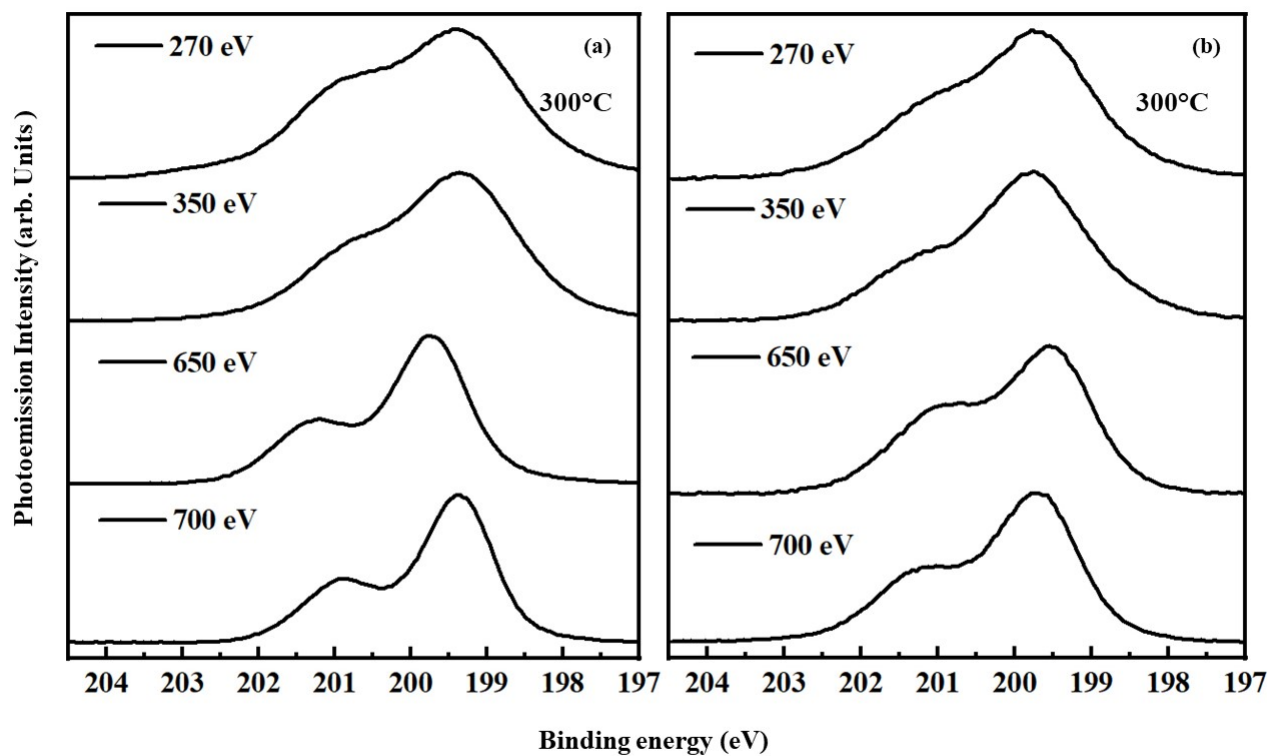


Figure SM1: Cl 2p core level spectra including data at 300 °C with different incident photon energies:(a) UHV cleaved spectra. (b) Air cleaved spectra.

16 3. Cr3p Spectra

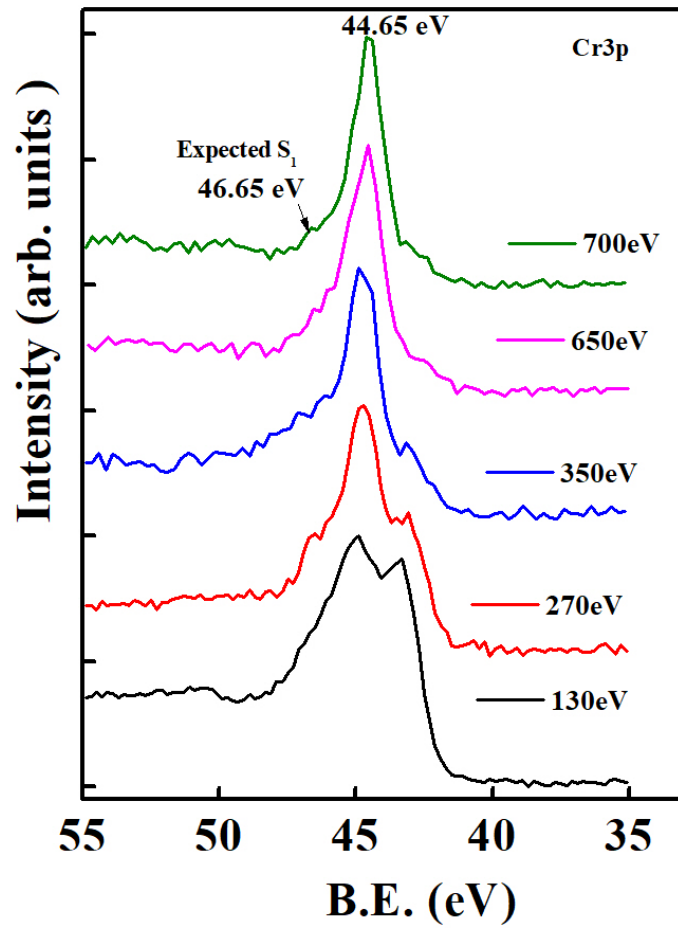


Figure SM2: Cr 3p core level spectra including satellite features at 150 °C with different incident photon energies.

17 **4. Valence Band**

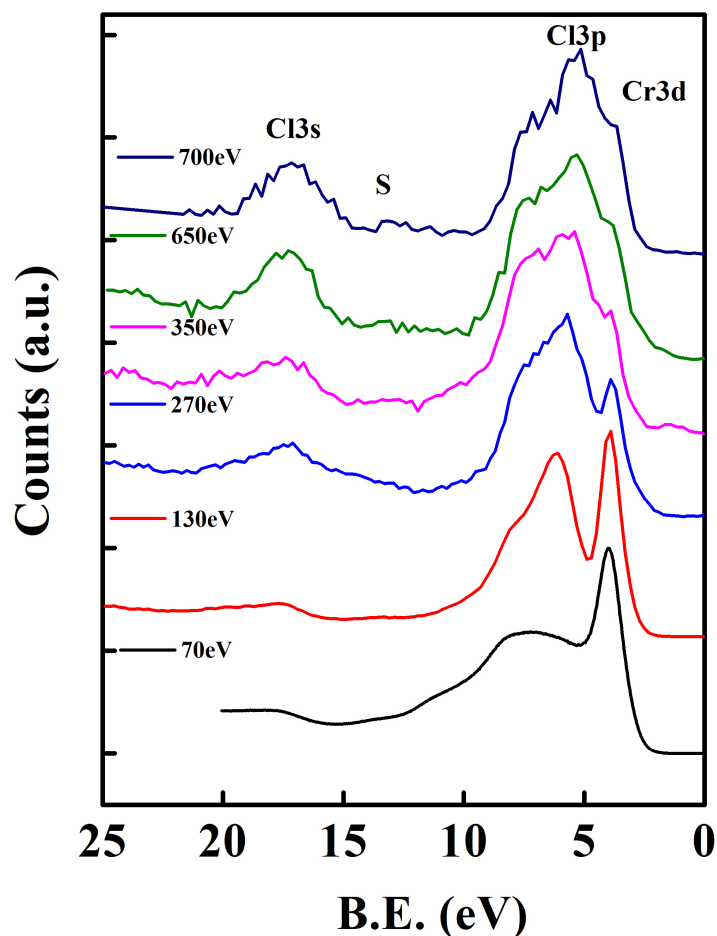


Figure SM3: VB spectra including satellite features at 150 °C.

18 Additional information on the correlation of the electronic structure can be obtained from the satellites energy as
19 shown in Fig SM 2 and Fig SM3 respectively. The satellite features are mainly related to the metal-ligand hybridization
20 and electron-electron interactions confirming the nature of CrCl₃ MH compound, while a trend towards charge transfer
21 is observed on the surface sensitive spectra when the satellite is missing.

22 **5. CTM4XAS (charge transfer multiplets for XAS/XPS) :**

23 The CTM4XAS program is used to analyze the charge transfer effect for 2p and 3p core level spectra of transi-
24 tion metals recorded by X-ray absorption (XAS), X-ray photoemission (XPS), or electron energy loss spectroscopy
25 (EELS). More details on the software can be found in ref [5]. We applied the theoretical model on Cr 2p and Cr 3p
26 in the most probable valence state i.e. (Cr⁺³). This calculation consists of set of appropriate parameters for charge

27 transfer, such as the crystal field (10Dq), the charge transfer energy (Δ), the average Coulomb interaction ($U^{dd} - U^{pd}$),
 28 and the energy splitting (e^g and T^{2g}). For Cr 2p, the Slater integral and spin-orbit coupling (SO) reduction were used
 29 as default (i.e., 100%), but for the Cr 3p core-level spectra, the value of the SO coupling reduction was kept at zero.
 30 Our spectra here consist of two principal components, one related to the multiplet effect (majority) and the other to
 31 charge transfer (minority). Consequently, two calculations were performed and compared to the experimental spectra.
 32 The linear combination of the two contributions as a whole is then shifted rigidly to fit the experimental energy.

33 6. Corrected XPS atomic sensitivity for photon energy:

34 To determine the surface composition of the exfoliated CrCl_3 flakes, the atomic sensitivity factor correction was
 35 calculated using the following formula, taking into account the variable kinetic energy of the photoemitted electrons:

$$\frac{S_{Cr}}{S_{Cl}} = \left(\frac{\sigma_{Cr}}{\sigma_{Cl}}\right) * \left(\frac{K.E._{Cr}}{K.E._{Cl}}\right)^{0.66} [6] \quad (\text{SM1})$$

36 For better understanding, we have presented a numerical example of the sensitivity correction at 700 eV photon
 37 energy:

$$\left(\frac{K.E._{Cr}}{K.E._{Cl}}\right)^{0.66} = \left(\frac{130}{500}\right)^{0.66} = 0.44 \quad (\text{SM2})$$

38 So, the corrected sensitivity ratio is :

$$\frac{S_{Cr}}{S_{Cl}} = 0.44 * 3.1 = 1.38 \approx 1.4 \quad (\text{SM3})$$

39 All atomic sensitivity ratios have been calculated in a similar way for other elements.

40 References

- 41 [1] D. Mastrippolito, L. Ottaviano, J. Wang, J. Yang, F. Gao, M. Ali, G. D'Olimpio, A. Politano, S. Palleschi, S. Kazim, et al., Emerging oxidized
 42 and defective phases in low-dimensional CrCl_3 , *Nanoscale Advances* 3 (2021) 4756–4766. doi:[10.1039/D1NA00401H](https://doi.org/10.1039/D1NA00401H).
- 43 [2] S. Kazim, R. Gunnella, M. Zannotti, R. Giovannetti, T. Klimczuk, L. Ottaviano, Determination of the refractive index and wavelength-
 44 dependent optical properties of few-layer CrCl_3 within the Fresnel formalism, *J. of Microscopy* 283 (2021) 145. doi:[10.1111/jmi.13015](https://doi.org/10.1111/jmi.13015).
- 45 [3] M. Serri, G. Cucinotta, L. Poggini, G. Serrano, P. Sainctavit, J. Strychalska-Nowak, A. Politano, F. Bonaccorso, A. Caneschi, J. Cava,
 46 R. Sessoli, L. Ottaviano, T. Klimczuk, V. Pellegrini, M. Mannini, Enhancement of the Magnetic Coupling in Exfoliated CrCl_3 Crys-
 47 tals Observed by Low-Temperature Magnetic Force Microscopy and X-ray Magnetic Circular Dichroism, *Adv. Mat* 32 (2020) 2000566.
 48 doi:[10.1002/adma.202000566](https://doi.org/10.1002/adma.202000566).
- 49 [4] S. Kazim, M. Ali, S. Palleschi, G. D'Olimpio, D. Mastrippolito, A. Politano, R. Gunnella, A. Di Cicco, M. Renzelli, G. Moccia, et al., Me-
 50chanical exfoliation and layer number identification of single crystal monoclinic CrCl_3 , *Nanotechnology* (2020). doi:[10.1088/1361-6528/
 51 ab7de6](https://doi.org/10.1088/1361-6528/ab7de6).

- 52 [5] E. Stavitski, F. M. De Groot, The CTM4XAS program for EELS and XAS spectral shape analysis of transition metal L edges, *Micron* 41
53 (2010) 687–694. doi:[10.1016/j.micron.2010.06.005](https://doi.org/10.1016/j.micron.2010.06.005).
- 54 [6] J. Yeh, I. Lindau, Atomic subshell photoionization cross sections and asymmetry parameters: 1 Z 103, *Atomic data and nuclear data tables* 32
55 (1985) 1–155. doi:[10.1016/0092-640X\(85\)90016-6](https://doi.org/10.1016/0092-640X(85)90016-6).